Available online at www.sciencedirect.com

SCIENCE DIRECT®

Coastal Engineering 51 (2004) 1105–1115

Coastal Engineering
An International Journal for Coastal, Harbour and Offshore Engineers

www.elsevier.com/locate/coastaleng

Density gradation in cross-shore sediment transport

R.L. Koomans[a,b,*], R.J. de Meijer[b]

[a]Medusa Explorations BV, P.O. Box 623, 9700 AP Groningen, The Netherlands
[b]Nuclear Geophysics Division, Kernfysisch Versneller Instituut, Rijksuniversiteit Groningen, 9747 AA Groningen, The Netherlands

Received 12 August 2003; received in revised form 2 July 2004; accepted 16 July 2004
Available online 11 September 2004

Abstract

One of the fundamental properties of a coastline is its sediment composition. Coastal sediments are rarely composed of one type of sediment. Due to these differences, the sediments are sorted on the beach and foreshore. The effect of density variations of the sediment on coastal sediment transport has been studied in a wave flume experiment. Two sands with an equal grain size distribution but with different densities (heavy minerals and quartz) have been used. Detailed measurements of profile evolution and of sediment composition have been used to assess the sediment transport rates for each sediment fraction.

The experiments show that the presence of heavy minerals in the sediment results in reduced erosion on the beach face; the breaker bar is smaller and its crest is more pronounced. The transport rates of different sediment fractions are not only determined by the availability at the bed. In the inner surf zone close to the beach, armouring occurs; in the inner surf zone close to the breaker bar, sediments are entrained more easily than expected. For effective armouring, the heavy mineral fraction in the bed should exceed a certain level. This threshold concentration is reached first close to the beach and extends later in seaward direction.

Keywords: Heavy minerals; Sediment transport; Armouring; Radionuclides

1. Introduction

Sedimentary coastlines have an attraction to many human beings. For many of them it is a place to relax, for others it is a way to earn a living, either on the dry part or from the regions offshore. Consequently, coastlines are often densely populated areas. These reasons make the presence and quality of a sandy coastline a valuable asset.

Due to a continuous relative rise of sea level and antropogenic structural interventions on the coastline (e.g. the building of harbours), erosion occurs. This leads to a change of the offshore profile, reduction in beach volume and, in the worst case, retreat of the protecting dune area. Therefore, authorities are often involved in an active maintenance of these geological systems. Because of the complex morphological coastal system and inherent natural variations, standardised methods to "cure" the problems are not

* Corresponding author. Medusa Explorations BV, P.O. Box 623, 9700 AP Groningen, The Netherlands. Fax: +31 505772534.
E-mail address: koomans@medusa-online.com (R.L. Koomans).

0378-3839/$ - see front matter © 2004 Elsevier B.V. All rights reserved.
doi:10.1016/j.coastaleng.2004.07.021

available. The European MAST-III project SAFE (performance of Soft beach systems And nourishment measures For European coasts), focussed on the problems of coastal retreat (Hamm et al., 2002). This project aimed at establishing new methodologies for solving present problems and tried to gain improved insight in the processes acting in the coastal zone for a better understanding for future protection. The work in this paper is part of the project SAFE and focuses on the improved understanding of sedimentary processes acting in the coastal zone.

One of the fundamental properties of a coastline is its sediment composition. Coastal sediments are rarely composed of one type of sediment. Grain sizes may vary from pebbles to coarse and fine sand, silt and clay; densities show variations from about 1.6 kg l^{-1} for certain carbonates to heavy minerals as dense as cassiterite (7.4 kg l^{-1}). Also, the shape of the grains can vary, e.g. from almost pure spheres to flat pebbles and flaky clays. Due to these differences, the hydrodynamic properties of the sediments will differ and the sediments are sorted on the beach and foreshore, leading to the observed grouping of materials.

Classification of sediments in their composition has for a long time been one of the few possibilities of deriving information on sediment transport processes in modern day environments. In geology this is, apart from observations on morphology, still the only way to derive the hydrodynamic conditions of the depositional environment. From the 1950s to the 1970s, a lot of work has been conducted on variations in sediment composition (Cordes, 1966; Eisma, 1968; Hand, 1967; Komar and Miller, 1974; Rao, 1957; Stapor, 1973). However, these analyses were time-consuming: samples have to be taken, and the precise work on the counting of heavy-mineral types, sieving of grain sizes, and measuring the rollability is a major effort, whilst separating heavy-mineral fractions with the toxic bromoform is expensive and unhealthy. The development of techniques to measure hydrodynamic conditions directly (e.g. current meters, wave-height measuring systems and equipment to measure suspended-sediment concentrations more precisely) caused a decreased interest in the elaborate analyses of sediment composition. Also, the development of numerical models resulted in a reduced interest in tedious and laborious measurements. With the increase of computer power and the better understanding of the modelling of sediment transport, models on sediment transport and morphological change started to incorporate variations in sediment characteristics. However, due to the lack of high-resolution data of sediment grading in time and space, it is difficult to validate these models and the importance of effects of sediment grading in the sediment transport processes is poorly understood.

This paper describes the effects of cross-shore density gradation on a coastal profile. To that end, the sorting of two sediment types with different densities has been studied in a wave-flume experiment. Detailed measurements of profile evolution and of sediment composition have been used to assess the sediment transport rates for each sediment fraction.

2. Experiment

To study the effects of selective transport, experiments were conducted in a wave flume (Scheldt flume, WL|Delft Hydraulics).

Two series of experiments have been conducted. Series A served as a reference study with uniform sediment. This series has been carried out on an initially plane beach, with a slope of 1 in 40, consisting of quartz (dune sand) with a median grain size of 129 μm (see Fig. 1). Series C aimed at

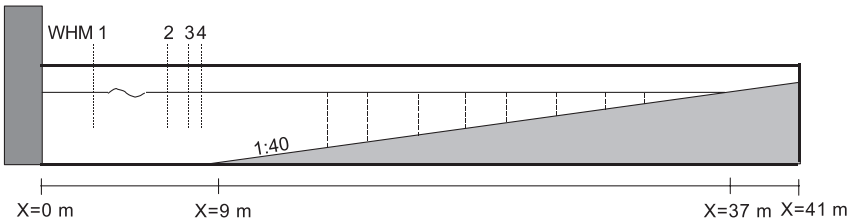

Fig. 1. Schematic setup of the experiment. The locations of wave-height meters (WHM) and positions of measuring verticals (vertical dashed lines) are indicated. The wave board moves within the area indicated by the grey box at the left.

Table 1
Initial geometry, sediment composition (in mass percentages) and total duration of the various experiments

Series	Initial geometry	Sediment composition	Wave duration (h:min)	Objective
A	plane, 1:40	quartz	29:36	reference test
C	plane, 1:40	60% quartz, 40% zircon	14:33	effects of density gradation on morphology

measurements of selective transport processes and profile evolution of density-graded sediments. The series started again from a 1 in 40 sloping plane bed, in which the upper 10 cm of the bed consisted of a mixture of ~60% quartz and ~40% zircon by mass (Table 1). The high concentration of the dense mineral zircon is not often found in nature, the mixture of 40% is chosen as an extreme to show the effect of the heavy mineral fraction.

Random waves were generated by a wave board equipped with an active wave-absorption system (Klopman, 1995), such that at the same time waves were generated and reflected waves were absorbed. The waves have been generated according to a second-order Stokes wave theory with the JONSWAP model. The JONSWAP spectrum has been developed to model growing storm waves with a limited fetch (Hasselmann et al., 1973) similar to conditions that occur on the North Sea. The incident wave conditions at deep water (water depth h=0.7 m) were characterised by wave height H_{m0}=0.17 m and the wave period T_p=2 s.

For the determination of the transport rates per sediment fraction, the profile evolution and changes in sediment composition have been measured. One of the possibilities of determining sediment composition in situ is via γ-ray measurements. In the past, these techniques have been applied regularly for studies of radioactive tracers in the field and in laboratory experiments (see, e.g. Pilon, 1963). With the development of improved hardware and analysis techniques, the measurement of variations in low-activity, naturally occurring radionuclides became possible (see, e.g. de Meijer et al., 1994; Tánczos, 1996). These naturally occurring radionuclides can be related to heavy-mineral concentrations (de Meijer et al., 2002; Tánczos, 1996) but also to concentrations of clay and sand (Venema et al., 1999). In this paper, measurements of natural γ-radiation have been used to determine heavy-mineral concentrations in the sediment (Koomans, 2000).

At selected time intervals (mostly the end of a day), the profiles are measured by a bed profiling system and with the MEDUSA system (de Meijer, 1998). The measurements were conducted along two parallel trajectories, each running 33 cm from one of the side-walls of the flume.

2.1. Sediment

The experiments focussed on the effect of density gradation in sediment transport. Therefore special attention was paid to the selection of the sediment types. In series A, quartz sediments have been used. In the experiments of series C, zircons with a higher density than quartz were added to the quartz sediment. To avoid hiding effects (Reed et al., 1999), the grain size of the zircons was similar to that of the quartz minerals. The dense mineral zircon is a reddish-coloured mineral and is considerably enhanced in radionuclide concentrations of ^{232}Th and ^{238}U. The large difference in radionuclide concentrations allows the radiometric measurement of zircon concentrations in the sediment with a high precision (de Meijer et al., 2002).

The sediment properties of the quartz and zircon used in series A and series C are summarised in Table 2 and Fig. 2. The grain-size distributions in Fig. 2 show that the d_{50} of zircon is 14 μm smaller than the d_{50} of the quartz but the shape of the distribution is

Table 2
The median grain size (d_{50}), 10 and 90 percentiles (d_{10} and d_{90}), settling velocity (w_{s50}), density (ρ) and activity concentrations (with external uncertainties) of ^{238}U and ^{232}Th for quartz and zircon

Sediment	d_{10} (μm)	d_{50} (μm)	d_{90} (μm)	w_{s50} (mm s^{-1})	ρ (10^3 kg m^{-3})	^{238}U (Bq kg^{-1})	^{232}Th (Bq kg^{-1})
Quartz	93	129	187	12	2.43 (0.10)	5.6 (0.3)	4.82 (0.15)
Zircon	83	115	153	27	4.4 (0.2)	12400 (400)	2300 (100)

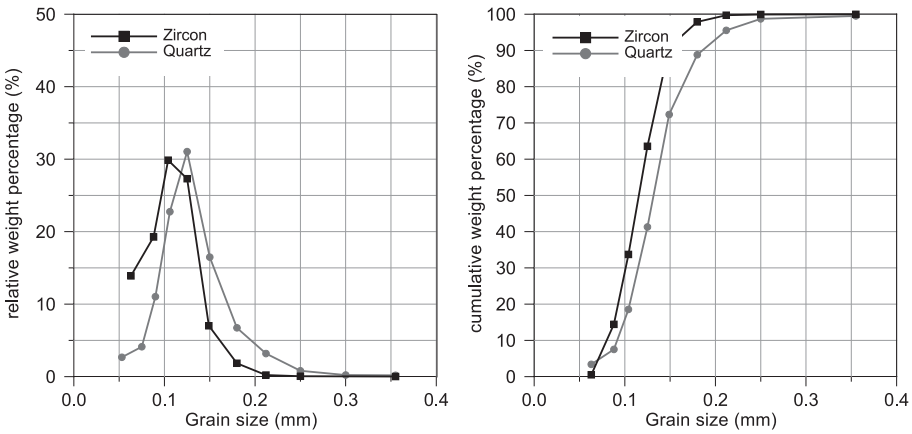

Fig. 2. Relative and cumulative grain-size distributions for quartz and zircon.

similar. The densities of both sediments (Table 2) were calculated after measuring the weight dry and underwater several times and the uncertainty represents the standard deviation in these measurements. The higher density of the zircon results in a settling velocity that is about twice the settling velocity of quartz. These settling velocities were measured in a settling tube. Visual observations on the sediments show that the shape and roundness are similar.

The MEDUSA system (Fig. 3) has been used to measure γ-radiation to derive the zircon concentration of the sediment bed. For these experiments, the MEDUSA system contains two casings (Fig. 3), one with the γ-ray detector and another with electronics. Both casings are placed on a PVC sledge to allow a smooth motion and to prevent sediment to pile up in front of the tubes (see Fig. 3).

3. Formulation of sediment transport

3.1. Volumetric sediment transport rates

Variations in bed height can be used to formulate a volume balance to determine the time-averaged sediment flux or transport rate $\langle q_v \rangle$ per unit width (W), in

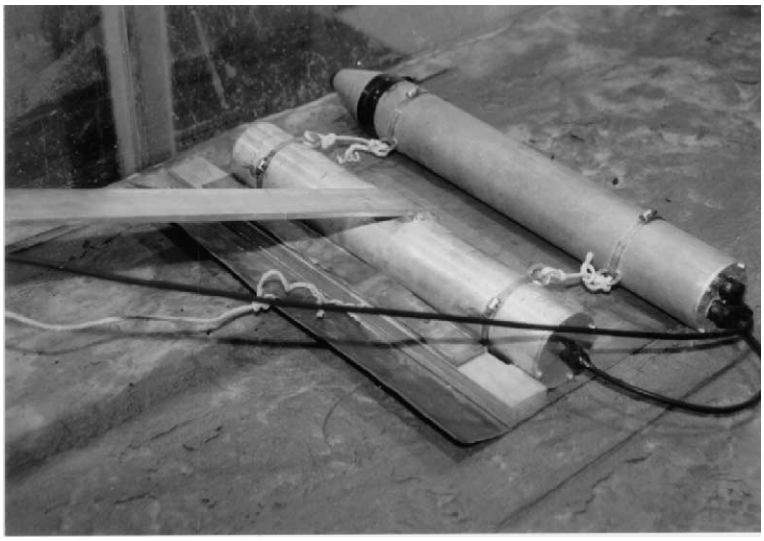

Fig. 3. The MEDUSA setup in the flume. The tubes are placed on a sledge to prevent sediment piling up in front of the detectors.

$m^3\ m^{-1}\ h^{-1}$ in a cross-section in the flume on location (x_0):

$$\langle q_v(x_0)\rangle = \frac{1}{W\Delta t}\int_{\text{offshore}}^{x_0} -\Delta z(x)\mathrm{d}x, \qquad (1)$$

with Δt the elapsed time (in hours) between the profile measurements.

To determine the mass fraction of quartz and zircon, the radiometric measurements of MEDUSA are analysed. Sediment samples from the final profile of the experiments have been used to validate the results of the measurements with the MEDUSA system (Koomans, 2000).

3.2. Mass transport rates

The concentration of zircon is used to calculate the time-averaged mass transport rate per sediment fraction of quartz or zircon $\langle q_q\rangle$ and $\langle q_z\rangle$, respectively, per unit width, in kg m^{-1} h^{-1} in a cross-section on location (x_0).

To calculate this mass transport per fraction of sediment, a mass-balance equation should be formulated based on the variations in profile evolution and the measured zircon concentrations of the bed. Therefore, the concentration of zircon should be known in a layer with a constant lower reference level. By doing so, mainly the sediments that actively participated in sediment transport are included. This layer can be considered similar to the "active layer" (see, e.g. Reed et al., 1999; de Meijer et al., 2002).

The mass change rate of zircon per unit width in cross-flume direction and in x-direction (kg m^{-2} h^{-1}) can then be determined by:

$$\Delta M_z = \frac{1}{\Delta t}\rho_z[(z+\mathrm{d}z)v_{z1} - zv_{z0}] \qquad (2)$$

with Δt the duration of the run (in hours), ρ_z the bulk density of zircon and v_{z1} and v_{z0} the volume fractions of zircon before and after the run, respectively. Similarly, the transported mass of quartz can be calculated from:

$$\Delta M_q = \frac{1}{\Delta t}\rho_q[(z+\mathrm{d}z)(1-v_{z1}) - z(1-v_{z0})]. \qquad (3)$$

The mass transport rates per unit width for the zircon fraction ($\langle q_z\rangle$, in kg m^{-1} h^{-1}) in a cross-section on location (x_0) follows then from:

$$\langle q_z(x_0)\rangle = \int_{\text{offshore}}^{x_0} -\Delta M_z(x)\mathrm{d}x. \qquad (4)$$

4. Results

4.1. Series A: quartz sand

Series A studies the morphological evolution of a barred beach system composed of uniform sediments: quartz. The wave conditions are similar to storm conditions. This experiment is the reference experi-

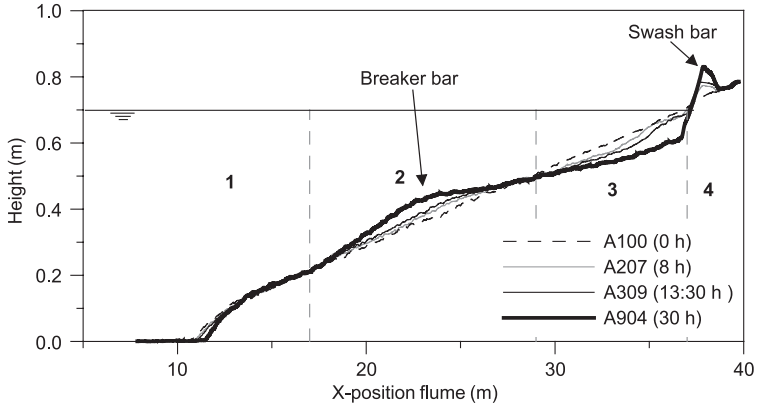

Fig. 4. Bed height measurements for different profiles of series A. The horizontal line indicates the water level in the experiment, the vertical dashed lines and the numbers point to a number of zones on the profile.

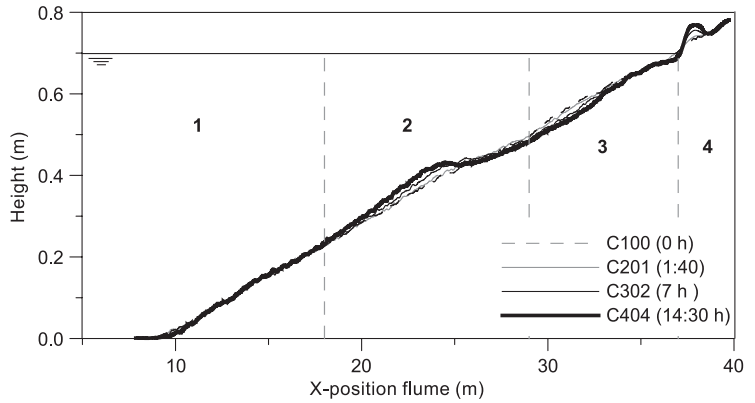

Fig. 5. Bed height measurements for different time intervals of series C. The horizontal line represents the time-averaged water level.

ment for series C that involves sediments graded on density.

Fig. 4 presents the evolution of bed height during four successive runs of series A. These results clearly show how a breaker bar (region 2) develops around x=20–25 m, corresponding to the location where the waves break. The crest of the breaker bar (the location of maximum curvature) progrades seaward to x=24 m for experiment A904. Landward of the breaker bar, the bed is eroded. This erosion starts at x=~30 m in experiment A207, but the location of maximum erosion progrades in the direction of the shoreline to x=36 m for experiment A904. The erosion in the inner surf zone (region 4, between breaker bar and water line) results in a steepening of the beach face at x=37 m. On the beach (x>38 m, region 5), a swash bar is formed.

4.2. Series C: quartz–zircon mixture

The profile evolution at various time intervals for series C (Fig. 5) shows the formation of a breaker bar between x=20 m and x=25 m. Landward of the breaker bar, the sediment bed is eroded. In a region just below the water line (34<x<37 m), the profile remains practically unchanged. Similar to the experiments of series A, a swash bar is formed just above the waterline.

Compared to the profile of the A-series (Fig. 6), the breaker bar in series C is narrower and its crest becomes more pronounced after a similar time interval. These results show that the admixture of zircons to quartz has an effect on the profile evolution: a considerable reduction of erosion occurring mainly in the area between the crest of the breaker bar and the

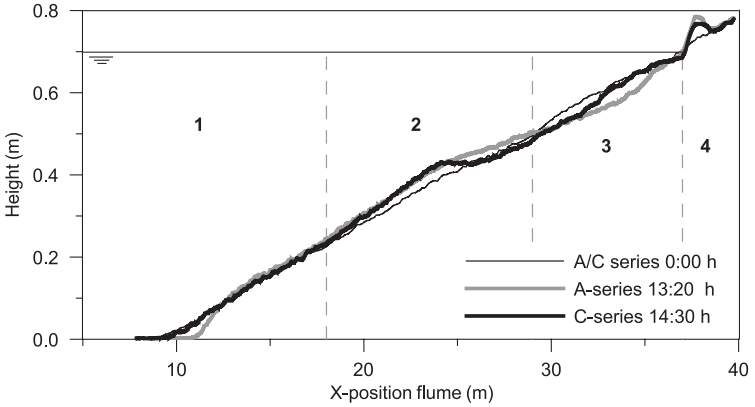

Fig. 6. Profile evolution for series A and series C after approximately 14 h.

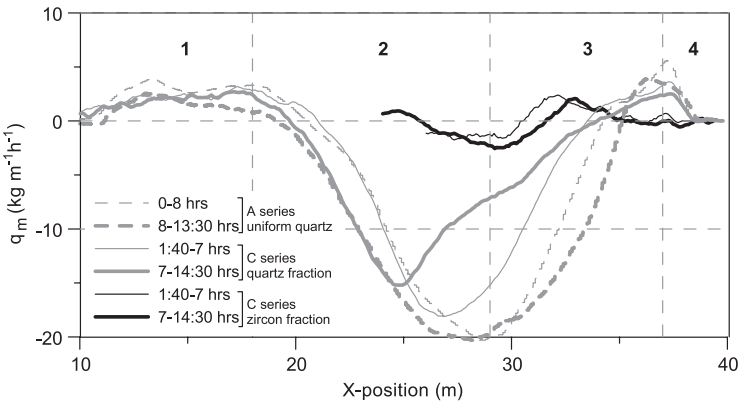

Fig. 7. Sediment transport rates of the quartz and zircon fraction in two time intervals of series C and sediment transport rates of similar time intervals of the A-series.

shore. The seaward side of the breaker-bar crest is similar for both experiments. At the toe of the profile (x<12 m), erosion in both series A is minimal. The difference in the final profiles in Fig. 6 is the result of a difference in the initial profile for both series.

In general, erosion is less for series C.

4.3. Mass transport rates per sediment fraction

Fig. 7 shows the sediment transport rates of the quartz and zircon fraction of series C and the transport rates of series A of similar time intervals.

If we compare the sediment transport rates of quartz and the quartz fraction for C201–C302, the transport rates are similar up to the crest of the breaker bar at x=26 m. For C302–C404, the sediment transport rates of quartz and the quartz fraction are similar for 10<x<15 m, but the transport rate of the quartz fraction is a factor of 2 larger for 15<x<20 m. In the region of the breaker bar, 20<x<25 m, sediment transport rates are similar. This indicates that mainly quartz sediments are transported offshore of the breaker bar. Visual observations and the measurements of the zircon concentration (Fig. 8) show that the zircon fraction is covered by these quartz sediments and, consequently, not available for sediment transport.

At more onshore locations, sediment transport rates of the quartz fraction are reduced with respect to sediment transport rates of the uniform quartz. This reduction is larger in the latter time interval. For the first time interval, the sediment transport gradients (the slope of the curve) are similar for 30<x<32 m. In the second time interval, the transport gradient of the quartz fraction is smaller than the transport gradient of

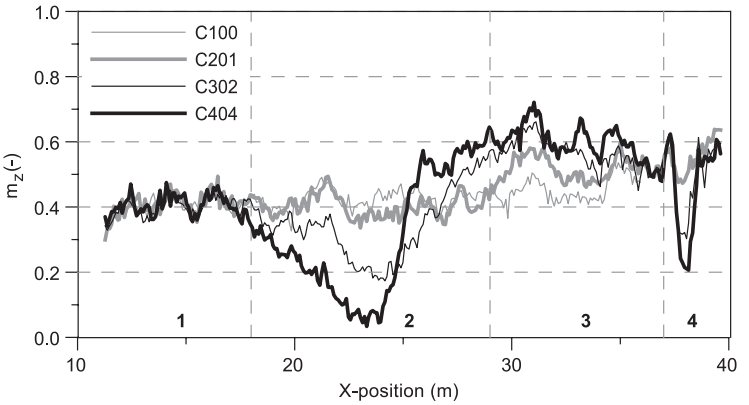

Fig. 8. Distribution of the zircon concentration in the upper 5 cm of the sediment for several runs of series C.

the uniform quartz for 30<x<35 m, pointing to a reduced erosion of quartz. For 26<x<30 m, the transport gradient is larger for the quartz fraction, indicating that the erosion of the fraction is larger in this region. Sediment transport rates on the beach (x>37 m) are similar for the uniform quartz and the quartz fraction.

The sediment transport of the zircon fraction is directed offshore for 25<x<31 m, similar to the direction of the quartz fraction, and is slightly larger for the last time interval. The maximum in the offshore-directed sediment transport rates is located around x=30 m and from there the transport rates decrease in onshore direction and reverse in sign at x=31 m. The subsequent maximum in onshore-directed sediment transport rates is located around x=32 m for both time intervals and the sediment transport rates decrease to q=0 towards the shoreline at x=35 m. The sediment transport rates of zircon in this region are opposite to the sediment transport rates of the quartz fraction. The two maxima in sediment transport rates of the zircon fraction indicate that zircons are deposited at x=30 m and x=32 m. At the swash bar at x=37 m, the sediment transport rates of zircon point to an onshore transport of zircon onto the swash bar.

In general, the sediment transport rates of the quartz fraction only deviate from the sediment transport rates of the uniform case of series A if a significant fraction of zircon is transported. If quartz and zircon both are eroded, erosion rates of the fractions are equal.

4.4. Zircon distribution

The variations in the mass transport rates per sediment fraction show that quartz and zircon behave differently. Since the zircon and quartz used in these experiments have a similar grain-size distribution, this selectivity in sediment transport reflects purely the effect of sediment density.

Since the erosion and accretion do not exceed 5 cm, the zircon concentrations are determined for the upper 5 cm of the sediment (Fig. 8). The initial concentration of zircon (C100) is not constant but shows small-scale variations and increases in shoreward direction. These variations are the result of selective processes during filling of the flume. Already in the first time interval, this distribution changes with distinct differences in the four morphological units of the coastal profile:

(1) The outer surf zone (x<18 m). Since the sediment transport rates in this region are small, sediments are not sorted and the zircon concentration remains constant.
(2) The breaker bar (18<x<25–29 m). The sediment transport rates of the two fractions show that mainly quartz is deposited on the seaward side of the breaker-bar crest located at x=25 m. Consequently, the concentration of zircon will decrease. At the landward side of the breaker-bar crest, quartz sediments are removed and zircons are deposited. Consequently, the concentration of zircons increases in this region. As we can observe in Fig. 8, the area of increased concentration of zircon moves offshore in time.
(3) The inner surf zone (25–29<x<37 m). In the inner surf zone, a complex interaction occurs between accretion and deposition of quartz and zircon sediments, but the average distribution of zircons is rather simple: the total zircon concentration in this region increases with a maximum around x=30 m. This zircon distribution points to the often-mentioned mechanism wherein quartz is removed from the inner surf zone, leaving zircons as a lag deposit (Komar and Wang, 1984; Stapor, 1973). The analysis of the transport rates of the sediment fractions shows a more sophisticated process: the simultaneous removal of quartz and zircon from the region around x=31 m, and the removal of quartz and deposition of zircon for 32<x<35 m result in similar zircon concentrations at the bed. This shows clearly that by looking at sediment composition only, transport rates for the sediment fractions cannot be derived accurately.
(4) The "dry" beach (x>37 m). On the swash bar, the concentration of zircons decreases with time. This is the result of the fact that mainly quartz sediments are deposited on the swash bar.

5. Assessment

Total sediment transport rates (q) are often described as the sum of transport rates for each

individual sediment fraction (q_i) (van Rijn, 1998):

$$q = \sum_i q_i, \tag{5}$$

In the modelling of graded sediment transport, it is often assumed that the volumetric fraction in the bed determines the transport rate of a sediment fraction and that these transport rates are not affected by other fractions. The sediment transport rate of a quartz fraction in the mixture ($q_{m,q}$) is the product of the sediment transport rate of uniform quartz ($q^*_{m,q}$) and the volume fraction (that parameterises the probability of pickup) in the bed (graph B in Fig. 9) (Reed et al., 1999; van Rijn, 1998):

$$q_{m,q} = v_q q^*_{m,q}. \tag{6}$$

Since the sediment transport rate of uniform zircon is in general smaller than the sediment transport rate of uniform quartz for equal hydrodynamic conditions, reducing the fraction of quartz will reduce the total net sediment transport rate:

$$q_m = (1 - v_q) q^*_{m,z} + v_q q^*_{m,q}. \tag{7}$$

Due to the larger sediment transport rate of the quartz fraction, this fraction is selectively removed from the upper (active) layer of the sediment. This results in the formation of a thin layer with a fraction of zircon that is higher than in the original sediment. The bed availability should therefore be determined from the volume fractions in the active layer. The thickness of the active layer is not well known. Several investigators have measured thicknesses ranging between two grain diameters (~0.5 mm) to values of 0.3 cm (Reed et al., 1999 and references therein). Experiments of selective transport of heavy minerals by Tánczos (1996) showed that the active layer thickness can be of the order of several cm.

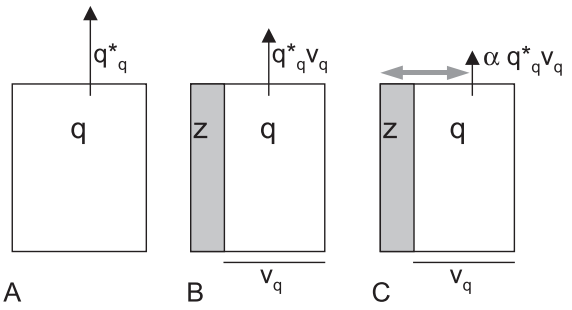

Fig. 9. Schematic presentation of the bed availability model (see Eq. (6)). In case of uniform quartz (q) bed, the total sediment transport rate is equal to the transport rate of the quartz fraction (A). If zircons (z) are added to the sediment, the transport rate of the quartz fraction is reduced due the reduction in the number of quartz grains per unit volume in the bed (bed availability model, B). If the sediment transport of the two fractions is not independent, the transport of the quartz fraction will be modified by a factor α (C). In case of armouring, α will be <1, in case of enabling, α will be >1.

If the sediment transport of the two fractions is not independent, the transport rates will be altered by a factor α (graph C in Fig. 9):

$$q_{m,q} = \alpha v_q q^*_{m,q}. \tag{8}$$

In case of armouring, α will be <1. When the transport rates are less reduced, α will be >1.

In the description of size-graded sediment, the assumption of independent transport rates of the fractions is not a priori valid due to hiding or exposure when smaller grains fall within the pores of the larger ones. Therefore, often a correction factor (e.g. Egiazaroff, 1965) is applied and the transport of the fraction is described by: $q_{m,q}=c\alpha v_q q^*_{m,q}$, with c as a correction factor. If this correction factor is not known properly, the effect of α cannot be estimated. Since the sediments in the experiments on density gradation have equal grain size, this effect is not of importance in the present study.

The mass transport rates of quartz in series C are compared to the transport rates for a uniform quartz bed multiplied with the quartz fraction (according to the bed-availability model) in Fig. 10A. These data have been used to calculate α (Fig. 10B). The results show that α varies along the profile and deviates from unity. In region 1, the bed-availability model underestimates onshore-directed sediment transport rates by a factor 1–2. This region is small for the first time interval ($16<x<19$ m) but has expanded in the second time series.

On the breaker bar (middle of region 2), the sediment transport rates are larger than expected ($\alpha>1$). The offshore limit of this region ($x=21$ m) is constant for both time series, but the seaward edge of this region moves offshore in time from $x=29$ m to

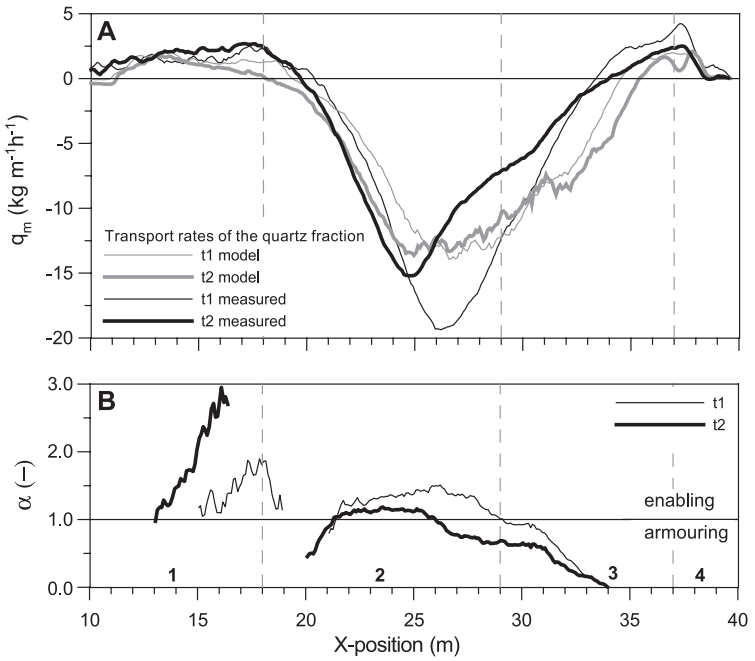

Fig. 10. (A) Sediment transport rates for the quartz fraction in series C compared with the sediment transport rates of series A multiplied with the fraction of quartz in the upper 5 cm of the sediment bed, for the first 7 h (t1) and the subsequent 7 h (t2). (B) Values of α (Fig. 9) calculated from the results in A.

x=26 m. Not only the width of this region decreases in time, but also the magnitude of the overestimation of the sediment transport rate decreases in the two time series; in t_2, α is almost equal to unity. Accounting for the "trend" that is present in the two measurements, the region of $\alpha>1$ will disappear.

In the inner surf zone (region 3), offshore-directed sediment transport rates for quartz are reduced ($\alpha<1$). For the first time interval, this occurs for region $29<x<34$ m. In the second series, the region of overestimation is broadened in offshore direction ($26<x<34$ m).

The results show that in case of density gradation, the transport rate of the sediment is not only determined by the availability at the bed. If we describe the sediment transport rates of the quartz fraction with a numerical model based on the assumption of Eq. (6), the breaker bar in series C would be too wide and erosion in the inner surf zone would be too large. The reduced erosion of quartz near the beach in series C cannot be fully attributed to the reduced availability of quartz in the sediment, but other factors are also important. The changes in bed composition result in the formation of an armour layer composed of zircon. This layer covers the quartz sediments and precludes quartz sediments from entrainment (Kuhnle and Southard, 1990; Reed et al., 1999). The increased effectiveness in armouring in the second time interval points to a process wherein the reduction of sediment transport only starts after a minimum concentration of zircon in the armouring layer. This observation is consistent with experimental results on density gradation in unidirectional flow (Kuhnle and Southard, 1990).

6. Conclusions

The Scheldt flume experiments show that the presence of heavy minerals in the sediment results in a beach face with reduced erosion; the breaker bar is smaller and its crest is more pronounced. In the experiments with a sediment mixture, the sediment transport rates are smaller and the sediment transport rates decrease faster in time than in the experiments with uniform quartz sediment.

The results of the experiments in the Scheldt flume indicate that the transport of sediment fractions is not only determined by the availability at the bed. In the inner surf zone close to the beach, armouring occurs; in the inner surf zone close to the breaker bar, sediments are entrained more easily than expected. In time, the extent of this latter region decreases and the region with armouring expands. Offshore of the breaker bar, the decreased availability does not affect sediment transport rates. It seems that for effective armouring, the zircon fraction in the bed should exceed a certain level. This threshold concentration is reached first close to the beach and extends later in seaward direction.

Acknowledgements

This work has been carried out under the EU programme Marine Science and Technology III under contract MAST3-CT95-0004. The experiments in the Scheldt flume were co-sponsored by the National Institute for Coastal and Marine Management/RIKZ of Rijkswaterstaat.

References

Cordes, E., 1966. Aufbau und bildungsbedingungen der schwermineralseifen bei skagen (Daenemark). Meyniana 16, 1–35.

de Meijer, R.J., 1998. Heavy minerals: from 'Edelstein' to Einstein. Journal of Geochemical Exploration 62 (1–3), 81–103.

de Meijer, R.J., et al., 2002. Gradation effects in sediment transport. Coastal Engineering 47 (2), 179–210.

de Meijer, R.J., Tánczos, I.C., Stapel, C., 1994. Radiometric techniques in heavy mineral exploration and exploitation. Exploration and Mining Geology 3 (No.4), 389–398.

Egiazaroff, I.V., 1965. Calculation of non-uniform sediment concentrations. Journal of the Hydraulics Division 91 (4).

Eisma, D., 1968. Composition, origin and distribution of Dutch coastal sands between Hoek van Holland and the island of Vlieland. Unpublished PhD thesis, University of Groningen, Groningen, 267 pp.

Hamm, L., et al., 2002. A summary of European experience with shore nourishment. Coastal Engineering 47 (2), 237–264.

Hand, B.m., 1967. Differentiation of beach and dune sands, using settling velocities of light and heavy minerals. Journal of Sedimentary Petrology 37 (2), 514–520.

Hasselmann, K., et al., 1973. Measurements of wind-wave growth and swell decay during the Joint North Sea wave project (JONSWAP). Deutsche Hydrographische Zeitschrift A8 (12).

Klopman, G., 1995. Active wave absorption, digital control systems for wave channels based on linear wave theory. H1222, WL|Delft Hydraulics.

Komar, P.D., Miller, M.C., 1974. On the comparison between the threshold of sediment motion under waves and unidirectional currents with a discussion of the practical evaluation of the threshold. Journal of Sedimentary Petrology 45, 362–367.

Komar, P.D., Wang, C., 1984. Processes of selective grain transport and the formation of placers on beaches. Journal of Geology 92, 637–655.

Koomans, R.L., 2000. Sand in motion: effects of density and grain size. PhD thesis, RUG, Groningen, 218 pp.

Kuhnle, R.A., Southard, J.B., 1990. Flume experiments on the transport of heavy minerals in gravel-bed streams. Journal of Sedimentary Petrology 60 (5), 687–696.

Pilon, J.J., 1963. Zandtransportmetingen met radioaktief tracermateriaal in Nederland. 11, Nota H-67-H, Waterloopkundige afdeling, Deltadienst-Rijkswaterstaat, Hellevoetsluis.

Rao, 1957. Beach erosion and concentration of heavy minerals. Journal of Sedimentary Petrology 27 (2), 143–147.

Reed, C.W., Niedoroda, A.W., Swift, D.J.P., 1999. Modeling sediment entrainment and transport processes limited by bed armoring. Marine Geology 154, 143–154.

Stapor, F.W., 1973. Heavy mineral concentrating processes and density/shape/size equilibria in the marine and coastal dune sands of the Apalachicola, Florida, region. Journal of Sedimentary Petrology 43 (2), 396–407.

Tánczos, I.C., 1996. Selective transport phenomena in coastal sands. PhD thesis, University of Groningen, Groningen, The Netherlands, 184 pp.

van Rijn, L., 1998. The effect of sediment composition on cross-shore bed profiles. In: Edge, B.L. (Ed.), International Conference on Coastal Engineering. ASCE, Copenhagen, pp. 1509–2495.

Venema, L.B., de Meijer, R.J., van Os, B., Gieske, J.M.J., 1999. In-situ characterisation of coastal and river sediment. In: Mocke, G.P. (Ed.), COPEDEC 99, Cape Town, South Africa, pp. 324–334.